

2010

Superconducting transition width under magnetic field in MgB₂ polycrystalline samples

C.C Wang
ISEM & Anhui University China

R Zeng
University of Wollongong, rzeng@uow.edu.au

Xun Xu
University of Wollongong, xun@uow.edu.au

S. X. Dou
University of Wollongong, shi@uow.edu.au

Follow this and additional works at: <https://ro.uow.edu.au/engpapers>



Part of the [Engineering Commons](#)

<https://ro.uow.edu.au/engpapers/1128>

Recommended Citation

Wang, C.C; Zeng, R; Xu, Xun; and Dou, S. X.: Superconducting transition width under magnetic field in MgB₂ polycrystalline samples 2010.
<https://ro.uow.edu.au/engpapers/1128>

Superconducting transition width under magnetic field in MgB₂ polycrystalline samples

C. C. Wang, R. Zeng, X. Xu, and S. X. Dou

Citation: *J. Appl. Phys.* **108**, 093907 (2010); doi: 10.1063/1.3488631

View online: <http://dx.doi.org/10.1063/1.3488631>

View Table of Contents: <http://jap.aip.org/resource/1/JAPIAU/v108/i9>

Published by the American Institute of Physics.

Related Articles

Pressure-induced tetragonal-orthorhombic phase transitions in CeRuPO

Appl. Phys. Lett. **102**, 051917 (2013)

Possibility of large superconducting gaps in the presence of quantum fluctuations

Low Temp. Phys. **38**, 1063 (2012)

Quantum phase slips in superconducting Nb nanowire networks deposited on self-assembled Si templates

Appl. Phys. Lett. **101**, 172601 (2012)

Superconductor-insulator transitions of quench-condensed films

Low Temp. Phys. **36**, 884 (2010)

A high energy “kink” in the quasiparticle spectrum as evidence of the importance of charge density fluctuations in the mechanism for high temperature superconductivity in cuprates

Low Temp. Phys. **36**, 716 (2010)

Additional information on J. Appl. Phys.

Journal Homepage: <http://jap.aip.org/>

Journal Information: http://jap.aip.org/about/about_the_journal

Top downloads: http://jap.aip.org/features/most_downloaded

Information for Authors: <http://jap.aip.org/authors>

ADVERTISEMENT



AIP Advances

Now Indexed in Thomson Reuters Databases

Explore AIP's open access journal:

- Rapid publication
- Article-level metrics
- Post-publication rating and commenting

Superconducting transition width under magnetic field in MgB₂ polycrystalline samples

C. C. Wang,^{1,2} R. Zeng,¹ X. Xu,¹ and S. X. Dou^{1,a)}¹*Institute of Superconducting and Electronic Materials, Wollongong University, Northfield Avenue, Gwynneville, New South Wales 2522, Australia*²*Laboratory of Dielectric Functional Materials, School of Physics and Material Science, Anhui University, Hefei 230039, People's Republic of China*

(Received 8 April 2010; accepted 10 August 2010; published online 4 November 2010)

A systematic study on the superconducting transition width as a function of the applied magnetic field was performed in polycrystalline MgB₂. A quantitative, yet universal relation between the two parameters was observed in all of the ceramics. It was found that the width decreases linearly with decreasing field in pure MgB₂ samples. Whereas, samples with boron and/or Mg atoms partially replaced by other elements show this linear relation in the temperature range below 0.7–0.8 of the superconducting transition temperature (corresponding to a field of about 2 T), at temperatures higher than this range, an abnormal upturn in the width was found. This upturn is ascribed to multiple superconducting transitions. A core-shell model is proposed to describe the multiple transitions. © 2010 American Institute of Physics. [doi:10.1063/1.3488631]

I. INTRODUCTION

The binary metallic MgB₂ superconductor has received wide attention in the past decade due to its transition temperature, which is several times higher than those of conventional metallic superconductors, giving the material tremendous promise for a wide range of large-scale applications. One of the most extensively investigated features of the superconductor relates to its electrical transport properties. Many authors¹ have pointed out that the high normal-state resistivity in MgB₂ samples results from the paucity of good electrical connectivity, which means a reduction in the effective cross-sectional area of the sample and thus a decrease in the critical current density (J_C). Rowell *et al.*^{1,2} suggested that the normal-state resistivity can be used as a gauge of the connectivity. They even derived a finite relationship, $J_C \propto 1/\Delta\rho_{300-50\text{ K}}$ (where $\Delta\rho_{300-50\text{ K}}$ is the difference between the resistivities at 300 and 50 K) in epitaxial thin films.² However, when we extend the study of resistivity to polycrystalline samples, the Rowell relation fails to quantitatively describe the connectivity for this system.³ Yamamoto *et al.*⁴ suggested an improved model by using the packing factor to evaluate the connectivity in polycrystalline MgB₂ based on a percolation method. On the other hand, since in the superconducting state, the superconducting transition broadening, as found in resistivity measurements in the presence of magnetic fields, contains important information related to the basic vortex-pinning mechanisms governing the critical current density. One may expect another resistivity-based relation in polycrystalline samples that can describe the electrical transport properties of MgB₂. Obviously, a thorough understanding of the resistive broadening is a prerequisite for this end. Although a large number of investigations have been performed on the resistive broadening of MgB₂, and it has been ascribed to a variety of causes, such as fluctuation effects, the

two gap superconductivity, surface superconductivity, and so on,⁵⁻⁷ most of these reports were qualitative. Therefore, quantitative studies on the resistive broadening become more imperative. In the present work, we report a quantitative investigation on this phenomenon by defining a superconducting transition width to describe the resistive broadening. The results show that there exists a universal relation between the superconducting width and the magnetic field in polycrystalline MgB₂ samples.

II. EXPERIMENTAL DETAILS

We have studied both pure and serially doped MgB₂ ceramic samples. Samples selected for presentation are numbered, and the corresponding compositions are listed in Table I. These samples were prepared by a diffusion reaction method. Starting powders of high-purity (99.999%) crystalline B with/without 10 wt % dopant for doped/pure samples were thoroughly mixed and pressed into pellets. The pellets were then sealed into an iron tube filled with Mg powder (99.8%) with the nominal composition ratio of B:Mg = 1:1.2. Finally, the iron tube was sintered at 850 °C for 10 h in a quartz tube furnace and then cooled down to room temperature. A high-purity Ar gas flow was maintained through-

TABLE I. Compositions of selected samples.

No.	Compound	Reference
1	Pure MgB ₂	This work
2	C-doped MgB ₂	This work
3	SiC-doped MgB ₂	This work
4	BN-doped MgB ₂	This work
5	Graphene-doped MgB ₂	This work
6	Si ₃ N ₄ -doped MgB ₂	This work
7	SiO ₂ -doped MgB ₂	This work
8	Al ₂ O ₃ -doped MgB ₂	This work
9	High-pressure sintered MgB ₂	Ref. 8

^{a)}Electronic mail: shi@uow.edu.au.

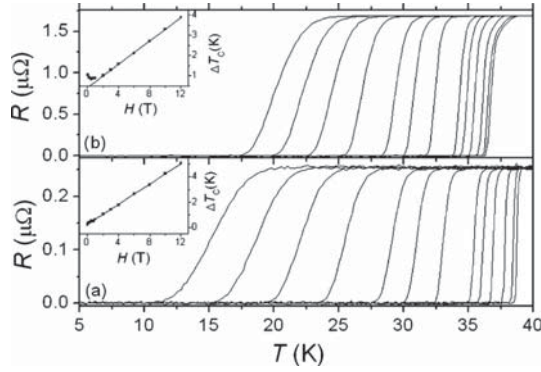


FIG. 1. R - T of (a) pure and (b) SiC-doped MgB_2 ceramic samples at $H=0, 0.1, 0.25, 0.5, 0.75, 1, 2, 3, 4, 6, 8, 10, 12$ T (increasing from right to left). The insets show the superconducting transition width, ΔT_C , as a function of H for the corresponding sample.

out the sintering process. The structural properties of the samples were examined by x-ray diffraction (XRD) and analyzed using Rietveld refinement. Resistive and magnetic measurements were carried out in a 14 T vibrating sample magnetometer. The resistance was measured by a standard four-probe technique. To substantially support our model, experimental data from a published reference on high-pressure sintered MgB_2 bulk (Ref. 8) are also introduced for comparison. The superconducting transition width was defined as $\Delta T_C = T_{90\%} - T_{10\%}$, where $T_{90\%}$ and $T_{10\%}$ are the temperatures corresponding to 90% and 10% of the resistivity at 40 K, respectively. The superconducting transition temperature, T_C , was defined by $T_C = (T_{90\%} + T_{10\%})/2$. In order to investigate the doping effect on the transition width, three SiC-doped MgB_2 samples were prepared by different methods aiming to adjust the doping level. Samples A and B were prepared by a diffusion reaction method but were sintered at 750 °C and 850 °C for 10 h, respectively. Sample C was prepared by an *in situ* reaction (mixed) method with sintering at 850 °C for 10 h. Details about the sample preparation were reported elsewhere.⁹

III. RESULTS AND DISCUSSIONS

A. The universal behavior of ΔT_C

Figure 1 shows typical examples of the temperature-dependent resistance (R - T) of (a) pure MgB_2 and (b) SiC-doped MgB_2 at various magnetic fields (H). The ΔT_C data deduced from the R - T curves are presented as insets in the corresponding panels. It is interesting to see that ΔT_C for the pure sample bears an excellent linear relationship with H over the whole measured magnetic field range, i.e.,

$$\Delta T_C = \Delta T_C(0) + kH, \quad (1)$$

where $\Delta T_C(0)$ is the transition width at $H=0$ T and k is a constant. The solid line shown in the inset of Fig. 1(a) is the result of a linear fit. The fit yields the values of the parameters $\Delta T_C(0)=0.2623$ K, $k=0.39662$ K/T, respectively, whereas for the SiC-doped sample, the linear behavior only holds when $H \geq 2$ T. The parameters $\Delta T_C(0)$ and k for this doped sample were found to be 0.42249 K and 0.28672 K/T, respectively. At fields lower than 2 T, an abnormal up-

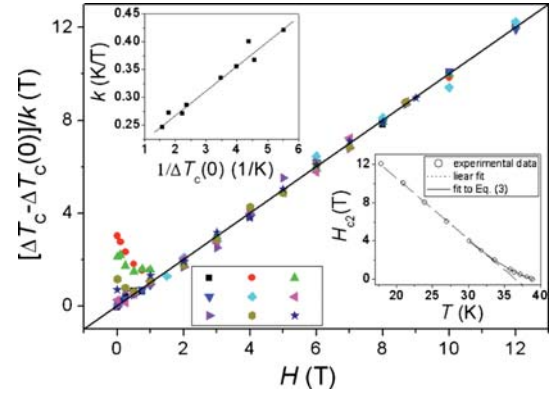


FIG. 2. (Color online) Scaling plot for data related to different compositions. The curves are numbered in accordance with the numbering of the compositions in Table I. The lower inset is the temperature-dependent H_{C2} . The dashed line is the linear fitting result, while the solid line is the fitting result based on Eq. (3). The upper inset shows the relationship between the parameters k and $\Delta T_C(0)$.

turn appears. The origin of the upturn will be discussed later.

To test whether this linear behavior holds for many ceramic samples, we examined samples doped with various dopants. If Eq. (1) is a universal expression for the samples, one can expect a scaling line by plotting $[\Delta T_C - \Delta T_C(0)]/k$ versus H . It is interesting to find that the scaling line truly exists. Figure 2 shows that the data points for all the samples fall perfectly on the scaling line with a slope of -1 in the field range above 2 T.

The linear behavior of ΔT_C can be well understood based on a percolation model,¹⁰⁻¹² which predicates the superconducting transition width as:

$$\Delta T_C = \frac{\sqrt{(\gamma^2 - 1)p_c^2 + 1} - 1}{(-\partial H_{C2}/\partial T)} H, \quad (2)$$

where H_{C2} is the upper critical field, γ denotes the anisotropy factor of the upper critical field, and p_c is the percolation threshold. For a given material, p_c is a finite value, γ is virtually a constant at temperatures sufficiently lower than the critical temperature T_C (corresponding to sufficiently large fields),¹³ and H_{C2} , determined as the 90% transition point on the R - T curves, is found to vary linearly with T for all samples at low enough temperatures. For example, the lower inset of Fig. 2 presents the H_{C2} values of the pure sample as a function of temperature, and a linear region is obvious at lower temperatures. When the temperature is higher than a crossover temperature at $\sim 0.8 T_C$, the curve deviates from linear behavior and displays a positive curvature. This upward curvature has been explained within the effective two-band model for type-II superconductors in the clean limit¹⁴ and can be well described by¹⁵

$$H_{C2}(T)/H_{C2}(0) = A(1 - T/T_C)^\alpha, \quad (3)$$

with the fitting parameters $H_{C2}(0) \times A$, T_C , and α found to be 28.853 T, 39.189 K, and 1.363, respectively. It is important to note that the crossover temperature in different samples was found to be around 0.7 to 0.8 T_C (corresponding to a field of about 2 T). This implies a universal H -linear behavior of ΔT_C in the low-temperature (high-field) range; while at

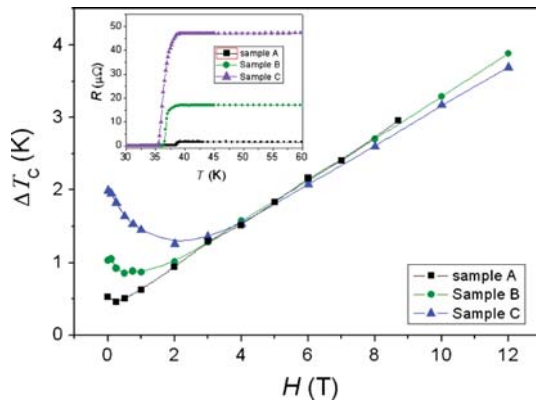


FIG. 3. (Color online) Superconducting transition width as a function of magnetic field for SiC-doped samples prepared by different methods as described in the text. The inset shows the R - T of these samples.

temperatures higher than the crossover temperature, the H -linear behavior no longer exists, since both γ and $\partial H_{C2}/\partial T$ show strong temperature dependence. This indicates that the superconducting broadening found in the high-field (low-temperature) range in polycrystalline samples is due to randomly oriented grains.

It is also worth noting that the percolation model proposes that $\Delta T_C(0)=0$, as indicated by Eq. (2), since the contribution of anisotropy tends to zero at zero field. However, the experimental results reveal the opposite case. This discrepancy might be because that the conclusions of the percolation model are based on the assumption that all the grains have identical properties.¹⁰ In fact, k was found to be well scaled by $1/\Delta T_C(0)$, as illustrated by the upper inset of Fig. 2, which implies that $\Delta T_C(0)$ tends to zero for sufficiently large k . We actually find that in highly dense samples, the value of $\Delta T_C(0)$ can be as low as 0.04 K. This fact indicates that the percolation model for a homogeneous system actually involves asymptotic behavior of practically inhomogeneous cases. This is understandable because the inhomogeneous factors such as porosity, cracks, etc., create additional broadening and give rise to a residual broadening at zero field. For a highly dense sample, the impacts of these factors can be greatly reduced, and therefore it is found that $\Delta T_C(0) \rightarrow 0$.

B. Origin of the low-field upturn of ΔT_C

We now turn our attention to the origin of the low-field upturn of ΔT_C . A careful examination of Fig. 1 reveals that the SiC-doped MgB_2 exhibits two R - T kinks, indicating two superconducting transitions, with the difference most profound at the lowest magnetic fields. The upturn in ΔT_C seems to be linked to the multiple superconducting transitions. To clarify this inference, we performed further experiments on three SiC-doped MgB_2 samples (sample A, B, and C) as indicated in the experimental details. The R - T curves of these samples are given in the inset of Fig. 3, from which we can see that all samples show the same onset superconducting transition temperature of 38.9 K. There are one and two R - T kinks, implying one and two superconducting transitions, in samples A and B, respectively. Although sample C does not

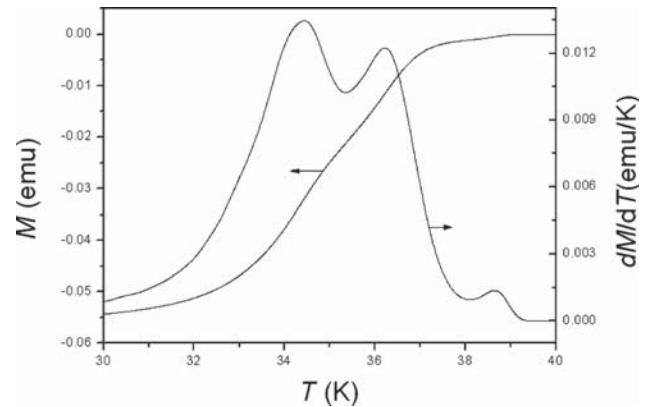


FIG. 4. Temperature dependence of magnetic susceptibility and its derivative for Sample C. Data were collected from a zero field cooled measurement at 0.01 T.

show two distinguishable kinks, both dc (see Fig. 4) and ac (not shown here) magnetic susceptibility (M) measurements revealed three superconducting transitions in this sample. The main panel of Fig. 3 shows the transition width, ΔT_C , as a function of H . It can be seen that the low-field upturn of ΔT_C becomes more and more notable as the number of superconducting transitions increases. This fact supports the above inference that the upturn is really linked with multiple superconducting transitions. In MgB_2 , two transitions have been occasionally reported, although the origin of this phenomenon is still unclear^{16–20} but three transitions are rarely reported. A conceivable origin of the multiple transitions is that the MgB_2 grains are separated into three phases with different T_C . This possibility suggests that clearly separated MgB_2 reflections should be observed in the XRD patterns. We, therefore, resort to the XRD results. A typical XRD pattern (symbols) and the refined profile (solid line) of sample C exhibiting notable multitransition was illustrated in Fig. 5. From which we can see that the MgB_2 phase is well-developed in the sample. In addition to some MgO impurity, no separated MgB_2 peaks were found. This result indicates that a mechanism other than the inhomogeneity of T_C among

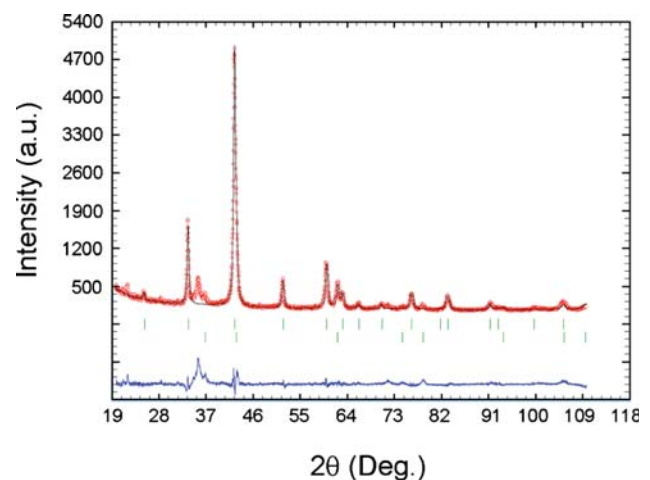


FIG. 5. (Color online) XRD pattern (symbols) with Rietveld refinement (solid line) for sample C. The lowest trace shows the difference between the measured and refined profiles.

TABLE II. Comparison of lattice parameters for pure MgB₂ and samples A, B, and C.

Sample (Å)	Pure	A	B	C
<i>a</i>	3.0847	3.0856	3.0845	3.0804
<i>c</i>	3.5237	3.5268	3.5282	3.5345

the MgB₂ grains underlies the multiple transitions. By careful examining the samples showing the low-field upturn of ΔT_C , we note that element replacement is a common feature for these samples. For example, in the SiC-doped and C-doped samples, the SiC-doping and C-doping allows C substitution for boron,²¹ while in the Al₂O₃-doped sample, Mg replaced by Al was widely reported.^{22,23} Although in SiO₂-doped sample, Si is doped into the MgB₂ lattice cell leading to the formation of Mg₂Si particles,²⁴ SiO₂ is regarded as a real impurity like MgO, which deteriorates the superconductivity by changing the microstructure and the grain connectivity.²⁵ The addition of Si₃N₄ also led to the formation of Mg₂Si, which is similar to the results of most other silicon compounds doping.²⁶ Whereas in BN-doped and graphene-doped samples, no element replacement was reported to the best of our knowledge. Based on these results, we herein present a core-shell model to describe the multiple transitions. Since the element replacement first occurs at the outermost parts of MgB₂ grains and gradually extends to the inner parts of the grains. It is natural to expect that, for not too long reaction time, the core of the grains still remains pure MgB₂ phase, which exhibits a higher superconducting transition, while the outer layers or the shell of the grains are the doped MgB₂ phase, which shows a lower transition temperature. For SiC-doped sample prepared by the mixed method, despite the C-doped phase, the whole grain may be embraced by the SiC phase, which introduces large thermal strain.²⁷ The thermal strain may lead to the shell further separates into two superconducting phases: the highly strained outmost layer of the shell has a transition temperature higher than that of the unstrained inner part of the shell.^{28,29} Therefore, three transitions can be observed in this sample.

The core-shell model is based on the fact that B and/or Mg atoms are partially replaced by C or other elements. Its validity is also supported by the XRD results. Taking the SiC-doped sample as an example, Table II lists the *a*-axis and *c*-axis lattice parameters of samples A, B, C, and pure MgB₂ for comparison. From this table, we can clearly see that when compared with the pure sample, the *c*-axis parameter is notably enlarged for all the SiC-doped samples. The *a*-axis parameter of sample B is virtually the same as that of the pure sample, while it shows a slight increase for sample A and a profound decrease for sample C. The change in the lattice parameters is a convincing evidence for atom replacement in the doped samples. It is important to point out that the *a*-parameter of sample A is larger than that of the pure sample. This is a different feature than that reported in literature,³⁰ which might be because that we use the diffusion method and crystalline B powder. Another reason might be

that C substituting for boron follows a two-step mechanism. That is, first C ions diffuse into the interstitial sites resulting in the expansion of both *a* and *c* parameters. Second, C ions start to substitute the boron sites mainly causing the enlargement of the *c*-parameter. A higher sintering temperature (sample B) favors the second step leading to the expanded *a*-parameter returns to its normal value and even becomes smaller than this value.

Based on the core-shell model, the above observed phenomena can be reasonably explained. First, the volume fraction of the shell depends on the sintering time and temperature. Higher sintering temperature favors the formation of the shell and causes a more profound upturn of ΔT_C , as has been already seen for samples A and B. Second, as the temperature decreases, the core is the first to go superconducting, and the first *R-T* kink occurs. However, the presence of the shell limits the formation of a percolation pathway until the shell becomes superconducting. Then a second *R-T* kink can be seen. Finally, and most importantly, the doped phase has enhanced flux pinning strength,²¹ which causes the *R-T* curve to move more slowly than that of the pure phase under low magnetic fields (also see Fig. 1). With the increasing field, the superconducting phases in the shell will be destroyed, as the flux enters this part first. Obviously, the superconducting transition width exhibits a large value, since it has contributions from multiple superconducting phases in the low-field range. The width goes to a minimum as the field becomes large enough to destroy the contributions from the shell, and then it will linearly increase with increasing field as the pure sample does. We therefore conclude that the origin of the low-field ΔT_C upturn is due to multiple superconducting transitions resulting from the replacement of B and/or Mg atoms by other elements.

IV. CONCLUSIONS

We have shown that there exists a universally linear relation between the superconducting transition width and the applied magnetic field in MgB₂ ceramics. This linear relation breaks down, and there is an abnormal low-field (high-temperature) upturn in the width in samples with B and/or Mg atoms have been partially replaced by other elements. This upturn was found to originate from multiple superconducting transitions that can be reasonably explained by a core-shell model.

ACKNOWLEDGMENTS

The authors are grateful for financial support from an Australian Research Council Discovery Grant (Grant No. DP0770205).

¹See, for example, J. M. Rowell, *Supercond. Sci. Technol.* **16**, R17 (2003).

²J. M. Rowell, S. Y. Xu, X. H. Zeng, A. V. Pogrebnyakov, Q. Li, X. X. Xi, J. M. Redwing, W. Tian, and X. Pan, *Appl. Phys. Lett.* **83**, 102 (2003).

³C. C. Wang, C. Wang, R. Zeng, and S. X. Dou, *J. Appl. Phys.* **108**, 023901 (2010).

⁴A. Yamamoto, J. Shimoyama, K. Kishio, and T. Matsushita, *Supercond. Sci. Technol.* **20**, 658 (2007).

⁵A. Sidorenko, V. Zdravkov, V. Ryazanov, S. Horn, S. Klimm, R. Tidecks, A. Wixforth, T. Kock, and T. Schimmel, *Philos. Mag.* **85**, 1783 (2005).

⁶T. Park, M. B. Salamon, C. U. Jung, M. S. Park, K. Kim, and S. I. Lee,

- Phys. Rev. B* **66**, 134515 (2002).
- ⁷T. Masui, S. Lee, and S. Tajima, *Physica C* **383**, 299 (2003), and references therein.
- ⁸A. K. Pradhan, Z. X. Shi, M. Tokunaga, T. Tamegai, Y. Takano, K. Togano, H. Kito, and H. Ihara, *Phys. Rev. B* **64**, 212509 (2001).
- ⁹S. X. Dou, V. Braccini, S. Soltanian, R. Klie, Y. Zhu, S. Li, X. L. Wang, and D. C. Larbalestier, *J. Appl. Phys.* **96**, 7549 (2004).
- ¹⁰M. Eisterer, M. Zehetmayer, and H. W. Weber, *Phys. Rev. Lett.* **90**, 247002 (2003).
- ¹¹M. Eisterer, C. Krutzler, and H. W. Weber, *J. Appl. Phys.* **98**, 033906 (2005).
- ¹²M. Eisterer, *Supercond. Sci. Technol.* **20**, R47 (2007).
- ¹³M. Zehetmayer, M. Eisterer, J. Jun, S. M. Kazakov, J. Karpinski, A. Wisniewski, and H. W. Weber, *Phys. Rev. B* **66**, 052505 (2002).
- ¹⁴S. V. Shulga, S. L. Drechsler, G. Fuchs, K. H. Müller, K. Winzer, M. Heinecke, and K. Krug, *Phys. Rev. Lett.* **80**, 1730 (1998).
- ¹⁵Y. Eltsev, S. Lee, K. Nakao, N. Chikumoto, S. Tajima, N. Koshizuka, and M. Murakami, *Phys. Rev. B* **65**, 140501(R) (2002).
- ¹⁶T. Nakane, K. Takahashi, T. Kuroda, and H. Kumakura, *Physica C* **468**, 1805 (2008).
- ¹⁷S. G. Lee, S. H. Hong, W. K. Seong, and W. N. Kang, *Supercond. Sci. Technol.* **22**, 064009 (2009).
- ¹⁸K. A. Yates, Z. Lockman, A. Kursumovic, G. Burmell, and N. A. Stelmashenko, *Appl. Phys. Lett.* **86**, 022502 (2005).
- ¹⁹I. Pallecchi, V. Ferrando, C. Tarantini, M. Putti, C. Ferdeghini, Y. Zhu, P. M. Voyles, and X. X. Xi, *Supercond. Sci. Technol.* **22**, 015023 (2009).
- ²⁰Y. Eltsev, *Physica C* **385**, 162 (2003).
- ²¹S. X. Dou, O. Shcherbakova, W. K. Yeoh, J. H. Kim, S. Soltanian, X. L. Wang, C. Senatore, R. Flukiger, M. Dhalle, O. Husnjak, and E. Babic, *Phys. Rev. Lett.* **98**, 097002 (2007).
- ²²J. S. Slusky, N. Rogado, K. A. Regan, M. A. Hayward, P. Khalifah, T. He, K. Inumaru, S. M. Loureiro, M. K. Haas, H. W. Zandbergen, and R. J. Cava, *Nature (London)* **410**, 343 (2001).
- ²³I. A. Ansari, M. Shahabuddin, K. A. Ziq, A. F. Salem, V. P. S. Awana, M. Husain, and H. Kishan, *Supercond. Sci. Technol.* **20**, 827 (2007).
- ²⁴X. F. Rui, Y. Zhao, Y. Y. Xu, L. Zhang, X. F. Sun, Y. Z. Wang, and H. Zhang, *Supercond. Sci. Technol.* **17**, 689 (2004).
- ²⁵O. Perner, W. Häbeler, J. Eckert, C. Fischer, C. Mickel, G. Fuchs, B. Holzapfel, and L. Schultz, *Physica C* **432**, 15 (2005).
- ²⁶C. H. Jiang, T. Nakane, and H. Kumakura, *Supercond. Sci. Technol.* **18**, 902 (2005).
- ²⁷R. Zeng, S. X. Dou, L. Lu, W. X. Li, J. H. Kim, P. Munroe, R. K. Zheng, and S. P. Ringer, *Appl. Phys. Lett.* **94**, 042510 (2009).
- ²⁸H. H. Wen, Z. X. Zhao, R. L. Wang, H. C. Li, and B. Yin, *Physica C* **262**, 81 (1996).
- ²⁹X. H. Zeng, A. V. Pogrebnikov, M. H. Zhu, J. E. Jones, X. X. Xi, S. Y. Xu, E. Werts, Q. Li, J. M. Redwing, J. Lettieri, V. Vaithyanathan, D. G. Schlom, Z. K. Liu, O. Trithaveesak, and J. Schubert, *Appl. Phys. Lett.* **82**, 2097 (2003).
- ³⁰C. Buzea and T. Yamashita, *Supercond. Sci. Technol.* **14**, R115 (2001).